International Journal of Pharmaceutics 664 (2024) 124641

Contents lists available at ScienceDirect

International Journal of Pharmaceutics

journal homepage: www.elsevier.com/locate/ijpharm

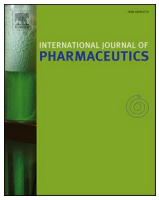

Production of liposomes by microfluidics: The impact of post-manufacturing dilution on drug encapsulation and lipid loss

Alessio Pittiu [a], Martina Pannuzzo [b], Luca Casula [a], Rosa Pireddu [a], Donatella Valenti [a], Maria Cristina Cardia [a], Francesco Lai [a], Antonella Rosa [c], Chiara Sinico [a], Michele Schlich [a,*]

[a] Department of Life and Environmental Sciences, University of Cagliari, Monserrato, CA 09042, Italy
[b] Data Science and Modelling, Pharmaceutical Sciences, R&D, AstraZeneca Gothenburg, Mölndal, Sweden
[c] Department of Biomedical Sciences, University of Cagliari, Monserrato 09042, CA, Italy

A B S T R A C T

Microfluidic mixing is recognized as a convenient method to produce liposomes for its scalability and reproducibility. Numerous studies have described the effect of process parameters such as flow rate ratios and total flow rate on size and size distribution of vesicles. In this work, we focused our attention on the effect of flow rate ratios on the encapsulation efficiency of liposomes, as we hypothesized that different amount of residual organic solvent could affect the retention of lipophilic drug molecules within the bilayer. In a further step, we investigated how the liposomes integrity and loading were impacted by different methods of solvent removal: direct dialysis and dilution & dialysis. Liposomes were prepared by rapidly mixing an ethanolic solution of lipids and a model drug with buffer in a herringbone micromixer, employing four different flow rate ratios (FRR, 4:1, 7:3, 3:2, 1:1). Quercetin, resveratrol and ascorbyl palmitate were used as model antioxidant drugs with different lipophilicity. Data showed that liposomes produced using lower flow rate ratios (i.e., with more residual ethanol) had lower encapsulation efficiencies as well as a more prominent loss of lipids from the bilayer following purification with direct dialysis. If the amount of residual ethanol was reduced to 5% (dilution & dialysis method), the lipids and drug leakage was prevented. Such effect was correlated with the drug aggregation propensity in different ethanol/water mixtures measured by molecular dynamics simulations. Overall, these results highlight the need to tailor the purification method basing on the molecular properties of the loaded drug to ensure high encapsulation and limit the waste of material.

1. Introduction

Liposomes are well-known drug delivery vehicles with a long-standing history of clinical success deriving from their peculiar properties, including biocompatibility, controlled drug release and ability to incorporate both hydrophilic and lipophilic compounds (Yusuf et al., 2023). Liposomes are composed of one or more phospholipid bilayers organized to form closed vesicles with size ranging from a few dozens of nanometers to several microns. Cholesterol is often added to the composition to increase phospholipid packing, reducing the bilayer permeability and improving the vesicle's stability (Briuglia et al., 2015). Many other molecules can be included in the liposomes' structure to achieve specific target product profiles. For instance, PEGylated lipids are usually employed to endow the vesicles with long-circulating properties (Gao et al., 2023; Pasut et al., 2015), co-solvents and edge activators promote flexibility (Carreras et al., 2020), targeting agents of different nature (from antibodies to small molecules) alter biodistribution and cell uptake (Agrawal et al., 2020; Cucca et al., 2018), and stimuli-responsive molecules modulate the release in specific environmental conditions (pH, redox status, light irradiation) (Abri Aghdam et al., 2019; Boruah and Chowdhury, 2022). In addition to the composition, the manufacturing method has a significant impact on critical quality attributes of liposomes, such as vesicle's size and drug encapsulation (Lombardo and Kiselev, 2022; Pisani et al., 2023). A vast scientific and patent literature on liposomes production methods is available, starting with the conventional and "historical" thin-film hydration techniques, through the direct sonication method, to the most modern approaches such as dual asymmetric centrifugation (Casula et al., 2023; Massing et al., 2008; Shah et al., 2020). Each method has different reproducibility, cost-effectiveness, and scalability: features that are often overlooked at the laboratory scale, but that became critical for the clinical transition of successful formulations. The quest for a continuous, reproducible, automatable, and robust production process resulted in the conceptualization and subsequent widespread adoption of microfluidic mixing to produce liposomes, as well as several other nano and micro-particles (Chiesa et al., 2022, 2021; Manghnani et al., 2022; Roces et al., 2019; Shah et al., 2020; Shepherd et al., 2021; Tiboni et al., 2021). In its essence, this method is based on the rapid mixing of a

* Corresponding author.
E-mail address: michele.schlich@unica.it (M. Schlich).

https://doi.org/10.1016/j.ijpharm.2024.124641
Received 23 May 2024; Received in revised form 16 August 2024; Accepted 23 August 2024
Available online 25 August 2024

water-miscible solvent containing dissolved lipids with an aqueous buffer in a microfluidic channel. During the mixing, the polarity of the fluid increases, reducing the solubility of lipids that spontaneously assemble into vesicular structures to minimize the contact of their hydrophobic alkyl chains with water (Zook and Vreeland, 2010). Hydrophilic and hydrophobic drugs can be efficiently entrapped in the forming vesicles by simply adding them into the water or the organic phases, respectively. One of the most important features of the microfluidic mixing method is the possibility to finely tune its operational parameters, including the total flow rate (TFR) and flow rate ratio (FRR). The TFR is the volume of formulation obtained in an arbitrary time unit, and the FRR is the volumetric ratio between aqueous and organic phases. These parameters describe the movement of fluids −which are governed by precision pumps- within the microfluidic channels (Carugo et al., 2016; Cui et al., 2004). The full control over the fluid dynamics led several research groups to explore the impact of FRR and TFR on colloidal parameters of liposomes, including the average diameter and polydispersity index (PDI) (Roces et al., 2020b, 2020a; Zhang and Sun, 2021). Some recent works also explored the possibility to predict those properties through machine learning approaches (Di Francesco et al., 2023; Rebollo et al., 2022). What emerged from experimental and modeling studies is that TFR has little impact on the dimensions of liposomes while FRR plays a major role. Generally, FRRs that are more markedly in favor of the aqueous phase led to the formation of smaller vesicles with a lower polydispersity index, because of the faster precipitation of lipids. The FRR value also dictates the amount of residual organic solvent after the microfluidic production: for example, a FRR of 3:1 (W/O) will result in liposomes with 25 % organic solvent. The concentration of organic solvent (generally ethanol, methanol, or isopropanol) has an impact on liposomes size when produced by a bulk method (ethanol injection) or by microfluidics, and its incomplete or delayed removal might affect the stability of vesicles (Carugo et al., 2016). Commonly used methods to remove alcohols from microfluidic-produced liposomes are dialysis and tangential flow filtration (TFF) (Table 1). In the dialysis method, a membrane of different materials and pore size separates the sample dispersion from a bulk aqueous solution, where the organic solvent can diffuse and be diluted to a non-critical concentration. In the diafiltration method, the sample is forced to circulate within a hollow fiber tubing that allows the diffusion of molecules smaller than a specific cutoff size. The solvents mixture filtered out of the tubing is replaced with an equal volume of aqueous buffer, and the process is continued until the organic solvent is completely removed (Tehrani et al., 2023). With the rise of interest towards the microfluidic fabrication of nanoparticles, some groups dedicated their effort to the development of continuous, microfluidic-based versions of these widely used purification methods (Hood et al., 2014; Shan et al., 2024). Another option to quickly decrease ethanol concentration is to dilute the liposomes mixture right after production. Different authors employed this straightforward approach to remove the organic solvent, but its impact on liposomes' properties was not specifically investigated (Webb et al., 2020, 2019). Conversely, it was demonstrated that a rapid dilution allowed more precise size control of nucleic acid-loaded lipid nanoparticles (LNPs) compared to dialysis (Hou et al., 2021; Kimura et al., 2020). As such, new microfluidic chips incorporating an in-line dilution channel are being developed by academic labs and companies specialized in microfluidic systems, with the aim of reducing the structural instability triggered by organic solvents (Shi et al., 2022).

Despite the huge interest around the microfluidic production of liposomes and the effect on colloidal properties, we realized that the impact of the purification method (i.e., dilution or dialysis) on encapsulation efficiency of drugs was never specifically investigated. This is a critical aspect especially when lipophilic compounds and low FRR are employed since high levels of organic solvent might promote solubilization rather than encapsulation of the drug.

In this work, we addressed this gap providing a head-to-head comparison between liposomes purified by dialysis with or without a preliminary dilution step. To provide a more complete overview, liposomes were prepared by microfluidics employing four different FRR, and compared to vesicles obtained by thin film hydration. Quercetin, resveratrol and ascorbyl palmitate were employed as model hydrophobic drugs with different lipophilicity. Finally, Molecular Dynamics (MD) simulations enabled to elucidate the mechanistic coupling between the behavior of the compounds in the different solvent mixtures and the resulting encapsulation yield.

2. Materials and methods

2.1. Materials

P90G was purchased from Lipoid GmbH (the analytical data of the batch employed for the experiments is reported in the Supporting Information); Resveratrol (RESV) was purchased from Galeno; 18:1 Liss Rhod PE was purchased from Avanti Polar; PBS salts, Cholesterol, Quercetin (QUE) and Ascorbyl palmitate (ASCP) were purchased from Merck. HPLC-grade solvents were purchased by Carlo Erba. All other products were of analytical grade.

Table 1
Workup strategies for removal of organic solvents after microfluidic production of liposomes. MeOH, methanol; EtOH, ethanol; iPA, isopropanol; PBS, phosphate buffer saline; TRIS, 2-Amino-2-hydroxymethyl-propane-1,3-diol; FRR, flow rate ratio; TFR, total flow rate; TFF, tangential flow filtration; RC, regenerated cellulose; mPES, modified polyethylenesulfone; HEPES, 4-(2-Hydroxyethyl)piperazine-1-ethanesulfonic acid; CE, cellulose ester.

Solvent	Aqueous phase	API	Microfluidic parameters	Dilution	Purification method	Ref
MeOH, EtOH	PBS pH 7.3, TRIS pH7.4	Ovalbumin	FRR 1:1—5:1 TFR 10–60 mL/min	YES (1:10)	TFF (mPES, 750 kDa)	(Webb et al., 2020)
MeOH, EtOH, iPA	PBS pH 7.3, TRIS pH 7.4	Ovalbumin and propofol	FRR 1:1—3:1 TFR 5—20 mL/min	YES (1:8.06)	TFF (mPES, 300/750 kDa)	(Webb et al., 2019)
EtOH	$(NH_4)_2SO_4$ pH 4.6	Acridine Orange HCl, Doxorubicin HCl	FRR 10:1 TFR 6 uL/min	NO	Custom chip dialysis (RC, 12—14 kDa), Dialysis (7 kDa)	(Hood et al., 2014)
EtOH	$(NH_4)_2SO_4$ pH 4.6	Doxorubicin	FRR 1:1 – 2:1 – 3:1—5:1 TFR 10—12- 20 mL/min	YES (1:1)	TFF (mPES, 500 kD)	(Roces et al., 2020b)
EtOH	TRIS pH 7.2	Propofol	FRR 1:1—5:1 TFR 0.5—6 mL/min	NO	Dialysis (3.5 kDa)	(Kastner et al., 2015)
EtOH	TRIS pH 7.2	Propofol, Ovalbumin	FRR 3:1 – 1:1 TFR 2 mL/min	NO	TFF (RC, 10 kDa)	(Dimov et al., 2017)
MeOH	PBS pH 7.3	Ovalbumin	FRR 1:1—3:1—5:1 TFR 5—20 mL/min	NO	TFF (mPES, 750 kDa)	(Forbes et al., 2019)
iPA	TRIS pH 7.4	None	Not reported	NO	Dialysis (cellulose, 3.5 kDa)	(Roces et al., 2016)

2.2. Preparation of liposomes

2.2.1. Preparation by microfluidics

Liposomes were prepared using a Herringbone Micromixer Chip (Microfluidic ChipShop) and a Syringe Pump (Chemyx Fusion 4000-x). The organic phase was composed of P90G (24 mg/mL), cholesterol (6 mg/mL) and one of the following drugs (QUE 0.5 mg/mL or RESV 0.5 mg/mL or ASCP 5 mg/mL) solubilized in ethanol. PBS (pH 7.4) was used as aqueous phase. Organic and aqueous phases were loaded in 5 mL syringes and mounted into the syringe pump. For liposomes preparation various flow rate ratios (FRR) were employed (4:1 – 7:3——3:2——1:1 W/O), while the total flow rate (TFR) was kept constant at 2 mL/min. The liposomal dispersions collected at the output of the microfluidic chip were processed following two alternative methods, described in paragraph 2.3.

2.2.2. Preparation by thin film hydration

Liposomes were also prepared by the thin film hydration method. Briefly, P90G (24 mg/ml), cholesterol (6 mg/ml) and one of the model drugs (QUE 0.5 mg/mL or RESV 0.5 mg/mL or ASCP 5 mg/mL) were dissolved in ethanol. The solution (0.4 ml) was placed in a round bottom flask and the solvent removed under vacuum. The thin film was hydrated with PBS (pH 7.4) for 30 min at 40 °C under mechanical stirring, then subjected to ultrasonication using a Soniprep 150 disintegrator (MSE, London, UK).

2.3. Liposomes post processing

Following production with microfluidic mixing, liposomes were post-processed using one of the following protocols: Direct Dialysis Method (DIR) or Dilution & Dialysis Method (DIL). Both methods served the purpose of removing the organic solvent and the un-entrapped drug from the formulations. In the case of DIR, liposomes were purified immediately after the production by means of dialysis using Pur-a-Lyzer (3.5 KDa) against 625x volumes of PBS (pH 7.4) for 2 h. In the case of DIL, liposomes after preparation were first diluted with PBS (pH 7.4) to reduce ethanol concentration to 5 % (v/v), then dialyzed as described above. Liposomes obtained by thin film hydration were purified from the un-entrapped drug using the DIR method.

2.4. Physico-chemical characterization

The average diameter and polydispersity index (PDI) of liposomes were measured by dynamic light scattering (DLS) using a Zetasizer Nano (Malvern Instrument, UK). Zeta-potential was determined using the Zetasizer Nano by means of the M3-PALS (Phase Analysis Light Scattering) technique. Liposomal dispersions were diluted 1:50 in MilliQ water for both diameter and Z-potential measurements. Unless otherwise stated, particle size, PDI and Z-potential are expressed as the average ± standard deviation (SD) of three experimental replicates.

2.5. Determination of the entrapment efficiency

Entrapment efficiency was determined measuring the absorbance of drugs (RESV, QUE, ASCP) with a plate reader (BioTek Synergy 4 Hybrid Multi-Mode Microplate Reader). Briefly, non-purified and purified liposomes were disrupted with EtOH to obtain a clear solution of the components. Drugs were quantified measuring the absorbance at defined wavelengths (λ_{RESV}=310 nm, λ_{QUE}=370 nm, λ_{ASC}=250 nm) and building calibration curves of drugs standard solutions in EtOH. The entrapment efficiency (EE%) was calculated as follows:

*EE%= drug amount in purified samples / drug amount in non-purified samples * 100.*

2.6. Lipid and liposomes recovery efficiency

Lipid quantification was performed by HPLC coupled with evaporative light scattering detector (ELSD). Liposomes processed by DIR method were disrupted with MeOH (1:10 v/v) and centrifuged for 5 min 5000 rpm. The supernatant was collected and analyzed. Liposomes processed through DIL method were frozen at −30 °C and lyophilized on a Buchi L200. The lyophilizate was resuspended in MeOH and centrifugated for 5 min 2380 G to yield a clear supernatant for analysis. The lyophilization step was necessary to have analytes in the dynamic range of the calibration curve. Aliquots (10 μL) of samples were injected into the Agilent Technologies 1100 HPLC system equipped with an Agilent Technologies Infinity 1260 evaporative light scattering detector (ELSD) (Palo Alto, CA). An Inertsil ODS-2 column (Superchrom, Milan, Italy) and MeOH as the mobile phase (at a flow rate of 1 mL/min) were used for the analyses of the mixture of phospholipids and cholesterol (Rosa et al., 2019). Recording and integration of the chromatogram data were carried out through an Agilent OpenLAB Chromatography data system. The identification of lipid components was performed using standard compounds, dissolved in MeOH before injection. Calibration curves of P90G phospholipids (mass on column: 5–25 μg) and cholesterol (mass on column: 1–10 μg) were constructed using standards and were found to be quadratic (with correlation coefficients > 0.995).

Liposome recovery was determined adding a fluorescent lipid (18:1 Liss Rhod PE) to the lipid mix at a concentration of 0.08 % (w/w) and measuring the fluorescence following disruption of liposomes with MeOH by microplate reader ($\lambda_{ex} = 560$, $\lambda_{em} = 585$).

2.7. Solubility tests

Saturated ethanolic solutions of each drug were prepared and kept under magnetic stirring at 25 ± 2 °C for 24 h. The dispersions were centrifugated for 20 min 19,000 G at 20 °C. The supernatant was then collected, appropriately diluted to operate in the dynamic range of the standard curves and analyzed by microplate reader as described above.

2.8. Computational simulation

For each of the three tested drugs (quercetin, resveratrol and ascorbyl palmitate), initial systems configurations were prepared by randomly placing 20 drug molecules along with ethanol and water solvents mixed at various ratios (13:87, 33:66, and 70:30) in a 7 x 7 x 7 nm cubic box using Packmol code (Martinez et al., 2009). Salt (0.15 M NaCl) and counterions were also included. The same systems were also prepared with an initial amount of 10 drug molecules and including 10 dipalmitoyl phosphatidylcholine (DPPC) molecules.

The Molecular Dynamics (MD) simulations were carried out using Desmond as implemented in Schrödinger software (Release 2023-4) and employing the OPLS4 force field parameters (Lu et al., 2021). The single point charge (SPC) model was chosen for water (Berendsen et al., 1981). Periodic Boundary Conditions (PBC) were applied in the three dimensions. After relaxation, all systems were simulated in an isothermal-isobaric (NpT) ensemble for 100 ns, using a reversible reference system propagator algorithms (RESPA) integrator (Tuckerman et al., 1992). A temperature of 300 K was kept constant using the Nosé–Hoover thermostat (Hoover, 1985; Nosé, 1984), with a relaxation time of 1.0 ps. The pressure was controlled using the Martyna–Tobias–Klein barostat (Martyna et al., 1994). A cut-off radius of 9.0 Å was used for short range interactions. The MD trajectories were analyzed using standard GROMACS tools (Van Der Spoel et al., 2005). Visual Molecular Dynamics (VMD) software was used for visualization and snapshots generation (Humphrey et al., 1996).

2.9. Statistical analysis

Results are expressed as the average ± SD. Multiple comparisons of

means (one-way ANOVA with post hoc Tukey HSD test) were used to substantiate statistical differences between groups, while Student's *t*-test was used to compare two samples. Data analysis was carried out with Excel (Microsoft, Redmond, WA, USA).

3. Results and discussion

3.1. Description of the production and workup phases

Liposomes loaded with the hydrophobic drug quercetin (QUE, logP 1.5) were prepared by microfluidic mixing in a staggered herringbone chip. The staggered herringbone microchip has two inlet channels, one for the organic phase containing lipids and one for the aqueous buffer, which converge in one central channel where the mixing happens, leading to the self-assembly of lipids into vesicular structures (Evers et al., 2018). In our setup, the flow rate ratios (FRR) between the aqueous buffer and the ethanolic phase containing lipids and QUE were varied to obtain four different production methods (Fig. 1**, Production**). Other process parameters such as total flow rate (TFR), lipid and drug concentration in the organic phase were kept constant. More specifically, FRR was set to the following values: 4:1, 7:3, 3:2 and 1:1 (PBS/ethanol), so that the resulting product coming out from the microfluidic chip consisted of lipid vesicles dispersed in PBS with 20, 30, 40 or 50 % ethanol, respectively. Except for some specific cases, residual solvents present at this stage must be completely removed to ensure stability of formed vesicles and to comply with guidelines on residual solvents in drug products (ICH, 2024). Such step can be defined as the workup phase. In general, exhaustive dialysis or tangential flow filtration (TFF) are employed to remove the organic solvent after microfluidic production of liposomes (Table 1). In addition to solvent elimination, both methods led to the removal of unentrapped drug from the sample. Dialysis is particularly common at the lab scale for its low cost and ease of use, while TFF allows for scalability and automatization (Dimov et al., 2017; Roces et al., 2020b). In this work, the workup of liposomes was carried out by two different methods (Fig. 1**, Workup**). The first method consisted of direct dialysis (DIR) of crude liposomes against PBS, while the second introduced a dilution step to reduce the amount of ethanol to 5 %, before proceeding with the dialysis (DIL). Among the literature examined (Table 1) only a limited number of reports includes a dilution step following the microfluidic process, but none addresses the impact of such procedure on the quality of liposomes with a head-to-head comparison.

In parallel to the microfluidic mixing, we also employed a conventional thin film hydration/ultrasonication method to prepare QUE-loaded liposomes. Such method served as a "zero-ethanol" control, as the formation of liposomes and encapsulation of drug molecules happens in the absence of organic solvents. As such, dialysis of these samples is not strictly required for stability or safety issues but could be employed to remove the unentrapped drug (i.e., to determine the encapsulation efficiency).

3.2. Physico-chemical characterization of QUE liposomes

Liposomes obtained by microfluidic mixing and purified with the DIR method showed hydrodynamic diameters ranging between 150–200 nm, with a trend towards larger vesicles when lower FRR was employed, and relatively narrow PdI (Fig. 2**A**). A similar dimensional trend could be observed for liposomes purified by the DIL method, that

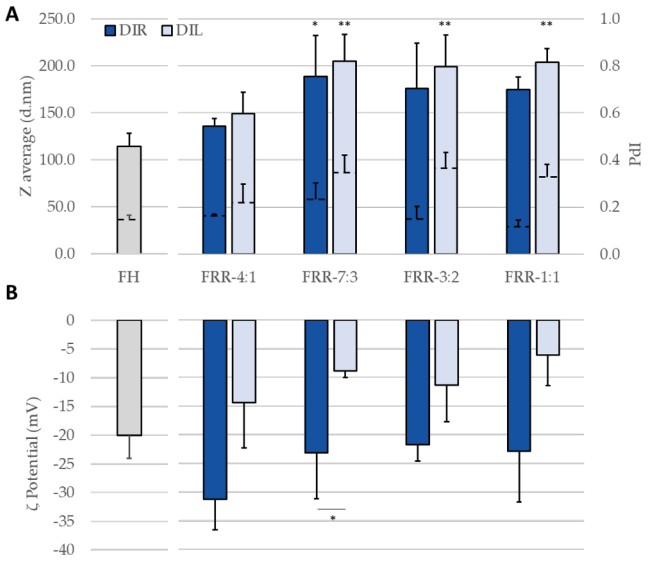

Fig. 2. Z Average (full columns) and polydispersity index (PdI, dashed lines) (**A**) and ζ-potential (**B**) of QUE liposomes produced by microfluidic mixing using different FRR and purified by DIR or DIL methods (average ± SD, n = 4). Data obtained from liposomes produced by film hydration/sonication method (FH) and purified by dialysis are also reported (average ± SD, n = 3). Symbols indicate statistically significant difference with liposomes prepared by film hydration (FH), or between groups linked by the lines (* $p < 0.05$; **$p < 0.01$, One-way ANOVA with post-hoc Tukey Test).

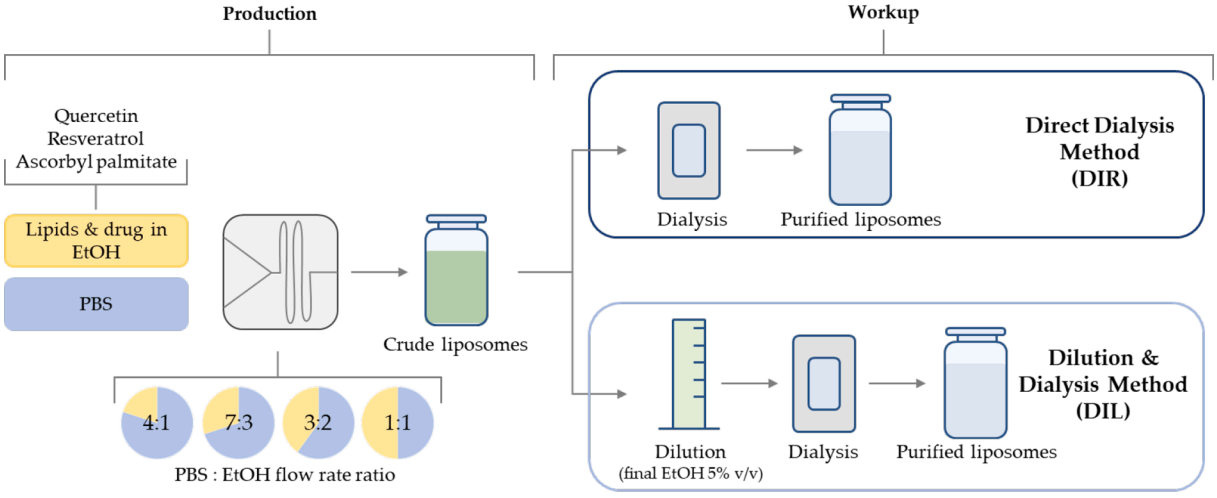

Fig. 1. Schematic of liposomes production and workup. The critical process parameters explored include flow rate ratios (FRR), type of drug (production phase) and methods for removal of solvent and unentrapped drug (workup phase).

led to an increased polydispersity. The thin film hydration/ultrasonication process yielded slightly smaller vesicles (114 ± 14 nm) with comparable size distribution. All formulations showed a consistent negative ζ potential in the range −20/–32 mV when purified by the DIR method, while the dilution led to an apparent, non-significant shift towards more neutral values (−6/-14 mV) (Fig. 2**B**). Results show that FRR plays a critical role. When nanocarriers are manufactured using high aqueous volumes, lipids tend to precipitate faster leading to smaller vesicles, as reported in other works (Carugo et al., 2016; Roces et al., 2020b). As regards the purification method, a previous report highlights that dialysis can significantly alter size and PdI of vesicles, and speculates that dilution can mitigate such effect (Roces et al., 2020a). Our results show that the dilution does not have a significant impact on hydrodynamic diameters but leads to an increase in polydispersity. This can be at least partly attributed to the method of dilution, that was performed by manual pipetting. The non-controlled, turbulent fluid mixing during dilution probably disturbed the assembly process producing a less homogenous sample. Considering a possible industrial development of liposomes purified by the DIL method, it would be important to optimize the dilution procedure to minimize the increase of PdI and yield a monodisperse vesicles population.

3.3. Entrapment efficiency of QUE liposomes

Liposomes produced with different FRR and purified by the two different workup processes were characterized in terms of QUE entrapment efficiency. Briefly, QUE was spectrophotometrically quantified after disruption of purified liposomes and results expressed as a percentage of QUE present in unpurified formulations. In the case of liposomes purified by the DIR method, the encapsulation efficiency gradually and significantly decreased when lower FRR was employed (Fig. 3). Lower FRRs mean that the crude mixture contains more ethanol (e.g, 50 % for FRR 1:1 vs 20 % for FRR 4:1), that promotes the solubilization of the hydrophobic drug rather than its incorporation in vesicular structures. The solubilized drug was then free to diffuse out of the dialysis bag, being removed from the formulation. On the other hand, in the DIL method the amount of residual ethanol was reduced to 5 % through the additional dilution step (Fig. 1, **solvent removal**). In this case, the encapsulation efficiency of liposomes did not change with FRR, confirming the role of the organic solvent in dictating the partition of the drug (Fig. 3). Of note, the encapsulation efficiency of liposomes produced by the film hydration method was not significantly different ($p > 0.05$) from that of liposomes produced by microfluidic mixing and purified by the DIL method, further corroborating this hypothesis.

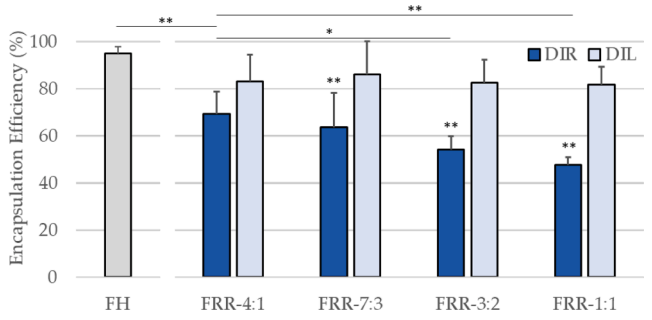

Fig. 3. Encapsulation efficiency of QUE in liposomes prepared by microfluidic mixing using different FRR and purified by DIR or DIL methods (average ± SD, n = 6). Data obtained from liposomes produced by film hydration/sonication method (FH) and purified by dialysis are also reported (average ± SD, n = 3). Symbols indicate statistically significant difference between DIR and DIL pairs at the same FRR, or between groups linked by the lines (* $p < 0.05$; **$p < 0.01$, One-way ANOVA with post-hoc Tukey Test).

3.4. Lipids recovery

The dependency of QUE encapsulation on the amount of residual ethanol prompted us to also monitor the loss of structural components of liposomes during the purification step. Both the mixture of phospholipids and cholesterol are indeed soluble in ethanol, and we hypothesized that lower FRR could be linked to a more pronounced loss of these components. To test this hypothesis, phospholipids and cholesterol in liposomal samples before and after workup were quantified by HPLC coupled with an ELSD detector. **Supplementary Figure 1** shows the chromatographic profile, obtained by HPLC-ELSD analysis, of cholesterol and phospholipids in liposomal samples. The chromatographic region of lipid components was assigned using standards of cholesterol, phosphatidylcholines, and P90G. The reversed phase mode allowed the separation of phospholipids based on ECN (=CN–2n, where CN is the number of acyl group carbons and n is the number of double bonds) (Rosa et al., 2019). P90G, a mixture of various phospholipids, showed a chromatographic profile characterized by two main peaks, corresponding to polyunsaturated phospholipids (ECN 28 and 30), and three minor peaks of phospholipids. The quantification of phospholipids in liposomal samples was performed considering the sum of the areas of all peaks (total area). As expected, the presence of large amounts of residual ethanol were linked to a higher loss of both phospholipids (Fig. 4**A**) and cholesterol (Fig. 4**B**), when liposomes are purified by the DIR method. Conversely, the DIL method allowed to recover > 77 % of phospholipids and > 82 % of cholesterol, without significant differences between formulations obtained using different FRRs. No loss of phospholipids or cholesterol was observed in the case of liposomes prepared by the thin film hydration method (data not shown).

3.5. Liposomes recovery

From lipids and drug quantification, it is clear that the DIR method is linked to a dramatic loss of components, especially when lower FRRs are employed in the manufacturing step. Such loss could potentially lead to a reduction in the number of liposomes present in suspension, or to the rearrangement of the components to yield smaller vesicles. This point was investigated by measuring the recovery of a fluorescently labelled lipid incorporated in the bilayer, as a tracker of the number of liposomes in suspension (Forbes et al., 2019). Although not suitable to obtain a direct measure of the number of liposomes in suspension, this technique can provide a reliable estimate of such value and was selected for its straightforwardness and cost-effectiveness. As expected, lower FRRs led to lower liposomes recovery when the formulations were subjected to a direct dialysis (DIR) (Fig. 5). In this context, recovery as low as 52 % could be observed when FRR 1:1 was employed. In line with what was observed with the hydrophobic drug, ethanol dissolves part of the lipids, diverting them from the self-assembly into vesicular structures and allowing their diffusion across the dialysis membrane. Conversely, the preliminary dilution (DIL) led to a drop in lipid monomer solubility, pushing the lipids to aggregate and form liposomes that are unable to cross the dialysis membrane. Therefore, the DIL method allowed a liposome recovery always higher than 92 %.

Such observation was corroborated by dynamic light scattering data, where the derived count rate of measures performed before/after dialysis was employed as an indicator to estimate the number of suspended vesicles (**Supplementary figure 2**). Finally, the dimensional analysis of the same samples proved that the dialysis does not have a significant impact on the average diameter of vesicles (**Supplementary figure 3**), supporting the conclusion that the loss of lipids upon DIR purification led to a reduction in the number of vesicles, rather than a reduction of size.

3.6. Impact of workup method on the recovery of other payloads

Results described in the previous sections highlight how the amount

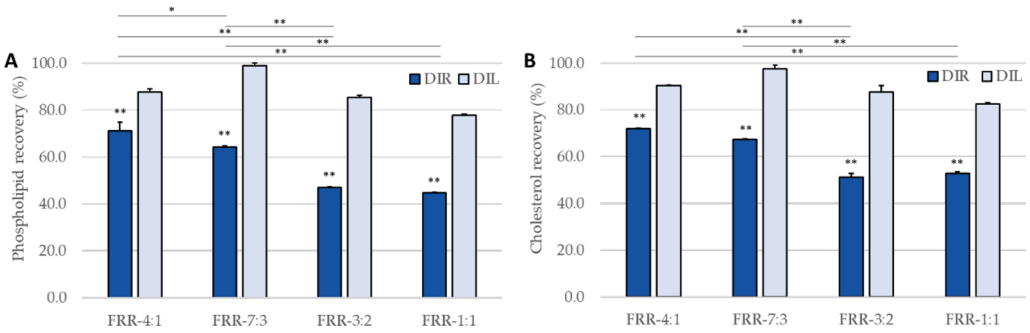

Fig. 4. Phospholipids (**A**) and cholesterol (**B**) recovery after purification of QUE liposomes with the DIR or DIL method, expressed as residual phospholipids or cholesterol detected by HPLC-ELSD (average ± SD, n = 2). Symbols indicate statistically significant difference between DIR and DIL pairs at the same FRR, or between groups linked by the lines (* $p < 0.05$; **$p < 0.01$, One-way ANOVA with post-hoc Tukey Test).

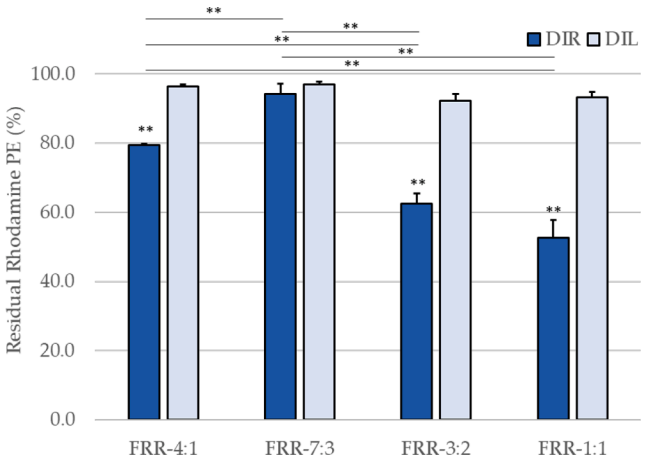

Fig. 5. Liposome recovery after purification of QUE liposomes with the DIR or DIL methods, expressed as % of residual Rhodamine PE detected by fluorescence spectroscopy (100 % = fluorescence of Rhodamine PE in liposomes before dialysis) (average ± SD, n = 3). Symbols indicate statistically significant difference between DIR and DIL pairs at the same FRR, or between groups linked by the lines (**$p < 0.01$, One-way ANOVA with post-hoc Tukey Test).

of residual ethanol in the formulation at the beginning of dialysis strongly influences the loss of lipids and QUE during purification. To assess if such observation applies to other hydrophobic drugs, liposomes with different payloads were produced and characterized. Specifically, resveratrol (RESV) or ascorbyl palmitate (ASCP) were loaded in liposomes, purified by the DIR or the DIL method. The physico-chemical characterization of liposomal dispersions is reported in Fig. 6. Both with RESV and with ASCP it was possible to observe a mild trend towards larger hydrodynamic diameters when lower FRR were employed. Conversely, the purification method did not have a significant impact on such parameters, with the exception of RESV liposomes produced with FRR 1:1, that were larger and more polydisperse when purified by the DIR method.

As concerns the encapsulation efficiency, both drugs showed a similar pattern to the one observed for QUE: (I) a direct correlation between FRR and encapsulation efficiency for liposomes purified by the DIR method, and (II) a constant encapsulation for liposomes purified by the DIL method regardless of the FRR (Fig. 7**A and B**). However, some differences in the behavior of the three drugs need to be highlighted. First, in the case of RESV, there was no significant difference between the DIR and DIL methods when FRR 4:1 and 7:3 were employed, meaning that residual ethanol concentrations between 5 % (DIL) and 30 % (DIR, FRR 7:3) had the same impact on the encapsulation efficiency (Fig. 7**A**). Second, vesicles prepared by the thin film method (0 % ethanol) had a significantly higher encapsulation efficiency, suggesting

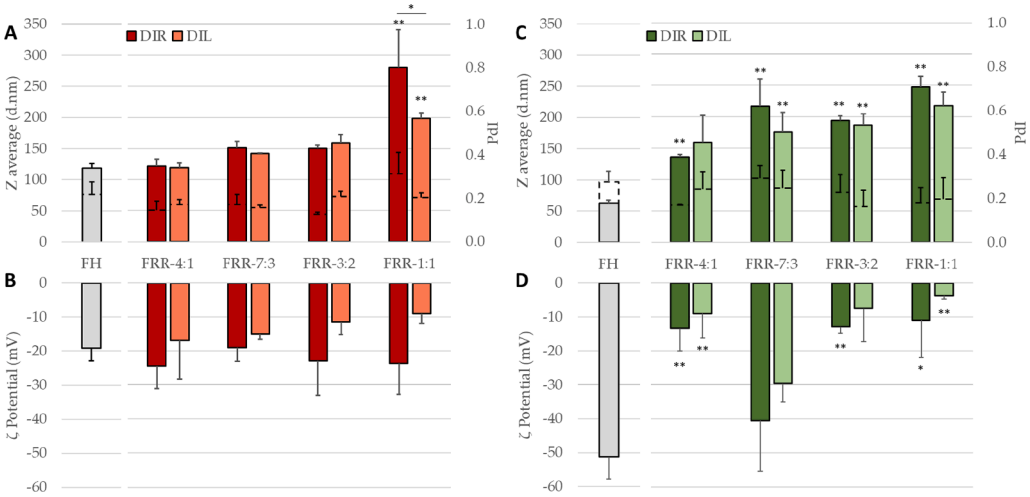

Fig. 6. Z Average (full columns) and polydispersity index (PdI, dashed lines) (**A**) and ζ-potential (**B**) of RESV liposomes produced by microfluidic mixing using different FRR and purified by DIR or DIL methods (average ± SD, n = 3). Z Average and polydispersity index (PdI) (**C**) and ζ-potential (**D**) of ASCP liposomes produced by microfluidic mixing using different FRR and purified by DIR or DIL methods (average ± SD, n = 3). Data obtained from liposomes produced by film hydration/sonication method (FH) and purified by dialysis are also reported (average ± SD, n = 3). Symbols indicate statistically significant difference with liposomes prepared by film hydration (FH), or between groups linked by the lines (* $p < 0.05$; **$p < 0.01$, One-way ANOVA with post-hoc Tukey Test).

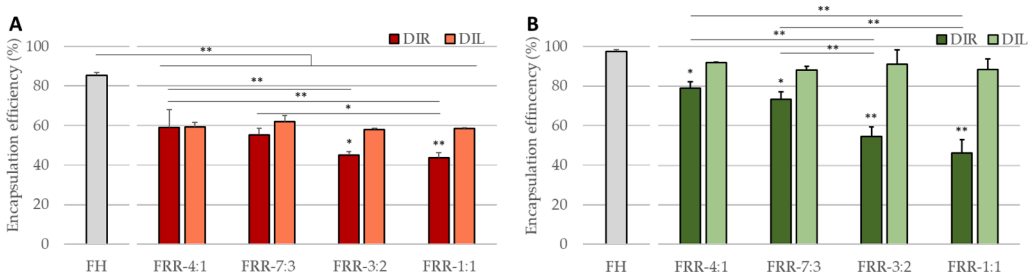

Fig. 7. Encapsulation efficiency of RESV (**A**) or ASCP (**B**) in liposomes prepared by microfluidic mixing using different FRR and purified by DIR or DIL methods (average ± SD, n = 3). Data obtained from liposomes produced by film hydration/sonication method (FH) and purified by dialysis are also reported (average ± SD, n = 3). Symbols indicate statistically significant difference between DIR and DIL pairs at the same FRR, or between groups linked by the lines (* $p < 0.05$; **$p < 0.01$, One-way ANOVA with post-hoc Tukey Test).

that even a small amount of organic solvent had a strong impact on RESV partition in the bilayers. This differs from what was observed for QUE (Fig. 3) and could be partly due to the higher ethanol solubility of RESV (76.68 ± 8.45 mg/ml) compared to QUE (29.97 ± 1.26 mg/ml). On the other hand, the effect of the workup method on ASCP encapsulation (Fig. 7**B**) was in line with what was observed for QUE. Also in this case, the DIR method led to a progressive loss of drug in presence of higher amounts of residual ethanol, while encapsulation efficiencies of liposomes purified by the DIL method, and liposomes produced by film hydration were similar ($p > 0.05$). As the solubility in ethanol of ASCP was determined to be 104.07 ± 19.24 mg/ml, this could not be the only parameter dictating the encapsulation behavior of drugs in these conditions. Other physico-chemical properties of the molecule, such as the presence of a large, linear hydrophobic domain prone to interact with alkyl tails of the phospholipids, are probably involved in dictating the interaction with lipid bilayers (Table 2).

3.7. Computational simulation

MD simulations of hydrophobic drugs were performed to investigate drug solution behavior in ethanol–water solvents mixed at different ratios. For all the three tested drugs, solubility decreased with an increased percentage of water in the mixture, thereby favoring drug aggregation (Fig. 8**A**). However, the aggregation propensity varied among the three drugs, as shown by the average cluster size formed in the different solvent mixtures (Fig. 8**B**). The aggregation propensity was highest for ASCP, followed by QUE and by RESV, whose molecules were not entirely aggregated even when the ethanol concentration in the mixture was low (13 %). This observation explains the encapsulation efficiency data of RESV liposomes: even a small amount of ethanol (5 % in the DIL method) is capable to partially solubilize RESV, leading to lower encapsulation in liposomes produced by microfluidic mixing compared to liposomes prepared by thin film hydration.

In a second step, DPPC lipids (serving as a mimic for a lipid vesicle) were added to the above ternary mixtures consisting of the API, ethanol and water (Fig. 9**A**). The lipid tended to phase separate already at high ethanol concentration, forming disordered and wide clusters. All the three drugs showed a stronger tendency to co-localize with the lipid phase at high water percentages compared to mixtures rich in ethanol, where drugs appear more freely dispersed (Fig. 9**B**). In the latter case, indeed, the drug interacts more with ethanol rather than with DPPC lipids.

Table 2
Physico-chemical properties of model drugs employed in this work. Molecular weights (MW), logP and topological polar surface area (TPSA) values were retrieved from pubchem.ncbi.nlm.nih.gov. Data on solubility in water were obtained from literature. Solubility in ethanol was measured at 25 ± 2°C (n = 3).

Drug	logP	MW	TPSA	Solubility in water	Solubility in EtOH	Structure
Quercetin (QUE)	1.5	302.23 g/mol	127 Å^2	< 60 μg/ml	29.97 ± 1.26 mg/ml	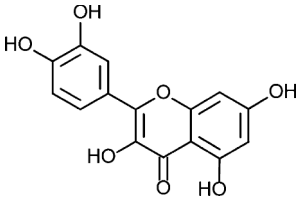
Resveratrol (RESV)	3.1	228.24 g/mol	60.7 Å^2	< 30 μg/ml	76.68 ± 8.45 mg/ml	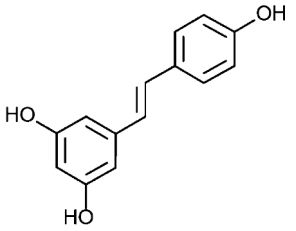
Ascorbyl palmitate (ASCP)	6.3	414.5 g/mol	113 Å^2	< 70 μg/ml	104.07 ± 19.24 mg/ml	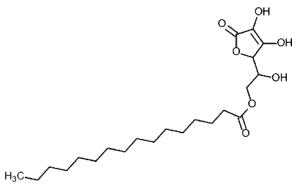

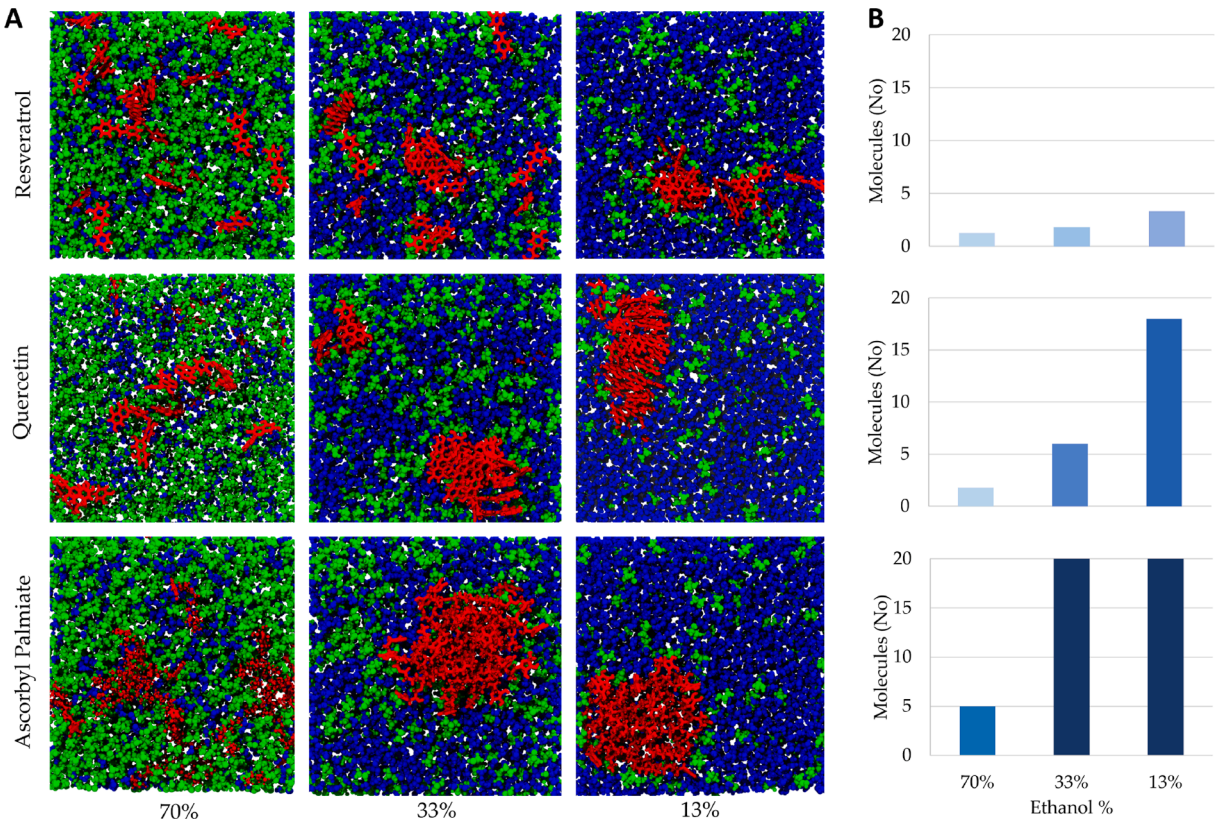

Fig. 8. Drug distribution in solvent mixtures at three different ethanol/water ratios (70 %, 33 % and 13 % ethanol from the left to the right, respectively). Snapshots were taken at the end of a 100 ns simulation. The drug is represented in red, ethanol molecules in green and water in blue. On the last column (**B**), the average drug cluster size is plotted against the percentage of ethanol in the solvent mixture.

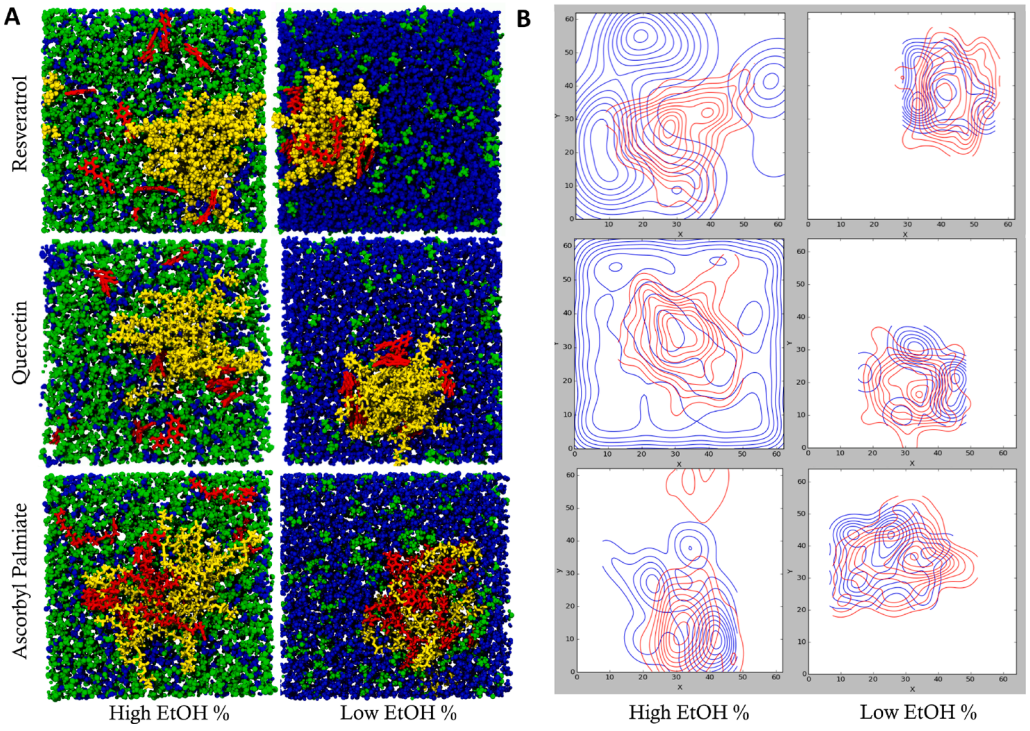

Fig. 9. Drug distribution in solvent mixtures at two different ethanol/water ratios (70 % and 13 % ethanol on the left and the right, respectively) and in the presence of DPPC lipids (in yellow). Snapshots were taken at the end of a 100 ns simulation. The drug is represented in red, ethanol molecules in green and water in blue (**A**). 2D distribution plotted as contour blue and red lines for the drug and DPPC lipids, respectively, at two different ethanol percentages in the solvent mixture (**B**).

Results from computational simulations of the quaternary mixtures support the description of the microfluidic mixing phases. In brief, liposomes are formed along the microfluidic mixer due to the rapid increase in solvent polarity, which implies a loss of lipid solubility and promotes the self-assembly of vesicles (Lim et al., 2020). The mixture at the outlet of the chip could be described as composed of two phases: one consists of phospholipid bilayers of newly formed vesicles, and one of the ethanol/water solution. Hydrophobic drugs, when exposed to increasing water concentrations along the mixing channel, tend to localize within the lipid bilayer or remain dissolved in the ethanol/water mixture. The partition coefficient for such equilibrium is influenced by the composition of the second phase, where more ethanol promotes the dissolution and more water disfavors it. The equilibrium is also dependent on other factors, such as the temperature and the ionic strength of the medium (i.e., environmental factors), or the drug physico-chemical properties, including its solubility in ethanol and structure (Table 2). What is interesting from the formulation development standpoint is that this is a dynamic system that can be modified after liposomes are formed. Indeed, the addition of water after the microfluidic mixing (as in the DIL method) strongly promotes the partition of lipophilic molecules in the bilayers. The obvious consequence of diluting the mixture is that the final product will have a lower concentration of the active drug. A lower concentration will in turn lead to less drug released per unit time (**Supplementary figure 4**), with possible consequences on the therapeutic dosing regimen. If needed, a concentration step could be implemented, but this would introduce an additional process with the relative costs.

4. Conclusions

In this work, the impact of liposomes dilution after microfluidic manufacturing on the encapsulation of hydrophobic drugs was systematically explored. Experiments using three different drugs showed that including a dilution step before the dialysis could improve the encapsulation efficiency, although to a different extent depending on the drug properties and on the amount of residual solvent. More specifically, liposomes manufactured at lower FRR (i.e., higher share of organic solvent) benefited the most from the dilution, while the impact became less relevant when higher FRRs were employed for the production. The same effect could be observed for liposomes' structural components, suggesting that care should be put in selecting the optimal workup method to avoid a significant loss of functional materials during the solvent removal. Computational simulations provided additional insights on the differences observed between the model drugs tested, showing that a higher aggregation propensity in aqueous mixtures is correlated with higher encapsulation efficiency, and that water-rich mixtures promote co-segregation of drug and lipid molecules (i.e., encapsulation). Dilution, however, might not be acceptable in case of liposomal drugs requiring a high dose in a limited volume (e.g., subcutaneous injections), unless a subsequent concentration process is introduced. In conclusion, the decision on whether to introduce a dilution step after microfluidic manufacturing should be carefully taken basing on the overall target product profile, including the sought encapsulation efficiency, final drug concentration and process cost and duration.

CRediT authorship contribution statement

Alessio Pittiu: Writing – original draft, Methodology, Investigation, Data curation. **Martina Pannuzzo:** Writing – original draft, Visualization, Investigation, Conceptualization. **Luca Casula:** Writing – review & editing, Validation, Methodology, Investigation. **Rosa Pireddu:** Investigation. **Donatella Valenti:** Investigation, Methodology. **Maria Cristina Cardia:** Writing – review & editing, Formal analysis. **Francesco Lai:** Visualization, Validation, Resources. **Antonella Rosa:** Writing – original draft, Methodology, Investigation, Formal analysis. **Chiara Sinico:** Validation, Supervision, Resources. **Michele Schlich:** Writing – review & editing, Writing – original draft, Supervision, Resources, Project administration, Funding acquisition, Conceptualization.

Declaration of competing interest

The authors declare that they have no known competing financial interests or personal relationships that could have appeared to influence the work reported in this paper.

Data availability

Data will be made available on request.

Acknowledgments

This work was partially supported by Sardegna Ricerche through the Proof of Concept in Biomedicine grant awarded to MS (REVIVE). MCC, FL and CS acknowledge the partial support of UniCA-Progetti biennali di Ateneo Finanziati dalla Fondazione di Sardegna 2021. MS thanks prof. Nicola Tirelli for the fruitful discussion on the results. The authors thank Lorenzo Picciau for the design of the graphical abstract.

Appendix A. Supplementary data

Supplementary data to this article can be found online at https://doi.org/10.1016/j.ijpharm.2024.124641.

References

Abri Aghdam, M., Bagheri, R., Mosafer, J., Baradaran, B., Hashemzaei, M., Baghbanzadeh, A., de la Guardia, M., Mokhtarzadeh, A., 2019. Recent advances on thermosensitive and pH-sensitive liposomes employed in controlled release. J. Control. Release 315, 1–22. https://doi.org/10.1016/j.jconrel.2019.09.018.

Agrawal, M., Saraf, S., Saraf, S., Dubey, S.K., Puri, A., Patel, R.J., Ajazuddin, R., Murty, V., Alexander, A., 2020. Recent strategies and advances in the fabrication of nano lipid carriers and their application towards brain targeting. J. Control. Release 321, 372–415. https://doi.org/10.1016/j.jconrel.2020.02.020.

Berendsen, H.J.C., Postma, J.P.M., van Gunsteren, W.F., Hermans, J., 1981. Interaction Models for Water in Relation to Protein Hydration. Intermolecular Forces. 331–342.

Boruah, J.S., Chowdhury, D., 2022. Liposome-azobenzene nanocomposite as photo-responsive drug delivery vehicle. Appl. Nanosci. 12, 4005–4017. https://doi.org/10.1007/s13204-022-02666-5.

Briuglia, M.L., Rotella, C., McFarlane, A., Lamprou, D.A., 2015. Influence of cholesterol on liposome stability and on in vitro drug release. Drug Deliv. Transl. Res. 5, 231–242. https://doi.org/10.1007/s13346-015-0220-8.

Carreras, J.J., Tapia-Ramirez, W.E., Sala, A., Guillot, A.J., Garrigues, T.M., Melero, A., 2020. Ultraflexible lipid vesicles allow topical absorption of cyclosporin A. Drug Deliv. Transl. Res. 10, 486–497. https://doi.org/10.1007/s13346-019-00693-4.

Carugo, D., Bottaro, E., Owen, J., Stride, E., Nastruzzi, C., 2016. Liposome production by microfluidics: Potential and limiting factors. Sci. Rep. 6, 1–15. https://doi.org/10.1038/srep25876.

Casula, L., Zidar, A., Kristl, J., Jeras, M., Kralj, S., Fadda, A.M., Zupančič, Š., 2023. Development of Nanofibers with Embedded Liposomes Containing an Immunomodulatory Drug Using Green Electrospinning. Pharmaceutics 15. https://doi.org/10.3390/pharmaceutics15041245.

Chiesa, E., Greco, A., Riva, F., Dorati, R., Conti, B., Modena, T., Genta, I., 2021. Hyaluronic acid-based nanoparticles for protein delivery: Systematic examination of microfluidic production conditions. Pharmaceutics 13. https://doi.org/10.3390/pharmaceutics13101565.

Chiesa, E., Bellotti, M., Caimi, A., Conti, B., Dorati, R., Conti, M., Genta, I., Auricchio, F., 2022. Development and optimization of microfluidic assisted manufacturing process to produce PLGA nanoparticles. Int. J. Pharm. 629, 122368 https://doi.org/10.1016/j.ijpharm.2022.122368.

Cucca, F., Caboni, P., Schlich, M., Bassareo, V., Corrias, F., Fadda, A.M., Frau, R., Lai, F., 2018. Systemic Administration of Orexin a Loaded Liposomes Potentiates Nucleus Accumbens Shell Dopamine Release by Sucrose Feeding. Front. Psychiatry 9, 1–11. https://doi.org/10.3389/fpsyt.2018.00640.

Cui, H.H., Silber-Li, Z.H., Zhu, S.N., 2004. Flow characteristics of liquids in microtubes driven by a high pressure. Phys. Fluids 16, 1803–1810. https://doi.org/10.1063/1.1691457.

Di Francesco, V., Boso, D.P., Moore, T.L., Schrefler, B.A., Decuzzi, P., 2023. Machine learning instructed microfluidic synthesis of curcumin-loaded liposomes. Biomed. Microdevices 25. https://doi.org/10.1007/s10544-023-00671-1.

Dimov, N., Kastner, E., Hussain, M., Perrie, Y., Szita, N., 2017. Formation and purification of tailored liposomes for drug delivery using a module-based micro continuous-flow system. Sci. Rep. 7, 1–13. https://doi.org/10.1038/s41598-017-11533-1.

Evers, M.J.W., Kulkarni, J.A., van der Meel, R., Cullis, P.R., Vader, P., Schiffelers, R.M., 2018. State-of-the-Art Design and Rapid-Mixing Production Techniques of Lipid Nanoparticles for Nucleic Acid Delivery. Small Methods 2, 1700375. https://doi.org/10.1002/smtd.201700375.

Forbes, N., Hussain, M.T., Briuglia, M.L., Edwards, D.P., te Horst, J.H., Szita, N., Perrie, Y., 2019. Rapid and scale-independent microfluidic manufacture of liposomes entrapping protein incorporating in-line purification and at-line size monitoring. Int. J. Pharm. 556, 68–81. https://doi.org/10.1016/j.ijpharm.2018.11.060.

Gao, Y., Joshi, M., Zhao, Z., Mitragotri, S., 2023. PEGylated therapeutics in the clinic. Bioeng. Transl. Med. 1–28 https://doi.org/10.1002/btm2.10600.

Hood, R.R., Vreeland, W.N., Devoe, D.L., 2014. Microfluidic remote loading for rapid single-step liposomal drug preparation. Lab Chip 14, 3359–3367. https://doi.org/10.1039/c4lc00390j.

Hoover, W.G., 1985. Canonical dynamics: Equilibrium phase-space distributions. Phys. Rev. A 31, 1695–1697. https://doi.org/10.1103/PhysRevA.31.1695.

Hou, X., Zaks, T., Langer, R., Dong, Y., 2021. Lipid nanoparticles for mRNA delivery. Nat. Rev. Mater. 6, 1078–1094. https://doi.org/10.1038/s41578-021-00358-0.

Humphrey, W., Dalke, A., Schulten, K., 1996. VMD: Visual Molecular Dynamics. J. Mol. Graph. 14, 33–38.

ICH, 2024. GUIDELINE FOR RESIDUAL SOLVENTS Q3C(R9) - Current step 4 version.

Kastner, E., Verma, V., Lowry, D., Perrie, Y., 2015. Microfluidic-controlled manufacture of liposomes for the solubilisation of a poorly water soluble drug. Int. J. Pharm. 485, 122–130. https://doi.org/10.1016/j.ijpharm.2015.02.063.

Kimura, N., Maeki, M., Sato, Y., Ishida, A., Tani, H., Harashima, H., Tokeshi, M., 2020. Development of a Microfluidic-Based Post-Treatment Process for Size-Controlled Lipid Nanoparticles and Application to siRNA Delivery. ACS Appl. Mater. Interfaces 12, 34011–34020. https://doi.org/10.1021/acsami.0c05489.

Lim, S.W.Z., Wong, Y.S., Czarny, B., Venkatraman, S., 2020. Microfluidic-directed self-assembly of liposomes: Role of interdigitation. J. Colloid Interface Sci. 578, 47–57. https://doi.org/10.1016/j.jcis.2020.05.114.

Lombardo, D., Kiselev, M.A., 2022. Methods of Liposomes Preparation: Formation and Control Factors of Versatile Nanocarriers for Biomedical and Nanomedicine Application. Pharmaceutics 14. https://doi.org/10.3390/pharmaceutics14030543.

Lu, C., Wu, C., Ghoreishi, D., Chen, W., Wang, L., Damm, W., Ross, G.A., Dahlgren, M.K., Russell, E., Von Bargen, C.D., Abel, R., Friesner, R.A., Harder, E.D., 2021. OPLS4: Improving force field accuracy on challenging regimes of chemical space. J. Chem. Theory Comput. 17, 4291–4300. https://doi.org/10.1021/acs.jctc.1c00302.

Manghnani, P.N., Di Francesco, V., Panella La Capria, C., Schlich, M., Miali, M.E., Moore, T.L., Zunino, A., Duocastella, M., Decuzzi, P., 2022. Preparation of anisotropic multiscale micro-hydrogels via two-photon continuous flow lithography. J. Colloid Interface Sci. 608, 622–633. https://doi.org/10.1016/j.jcis.2021.09.094.

Martinez, L., Andrade, R., Birgin, E.G., Martinez, J.M., 2009. Packmol: A Package for Building Initial Configurations for Molecular Dynamics Simulations. J. Comput. Chem. 30, 2157–2164. https://doi.org/10.1002/jcc.21224.

Martyna, G.J., Tobias, D.J., Klein, M.L., 1994. Constant pressure molecular dynamics algorithms. J. Chem. Phys. 101, 4177–4189. https://doi.org/10.1063/1.467468.

Massing, U., Cicko, S., Ziroli, V., 2008. Dual asymmetric centrifugation (DAC)-A new technique for liposome preparation. J. Control. Release 125, 16–24. https://doi.org/10.1016/j.jconrel.2007.09.010.

Nosé, S., 1984. A unified formulation of the constant temperature molecular dynamics methods. J. Chem. Phys. 81, 511–519. https://doi.org/10.1063/1.447334.

Pasut, G., Paolino, D., Celia, C., Mero, A., Joseph, A.S., Wolfram, J., Cosco, D., Schiavon, O., Shen, H., Fresta, M., 2015. Polyethylene glycol (PEG)-dendron phospholipids as innovative constructs for the preparation of super stealth liposomes for anticancer therapy. J. Control. Release 199, 106–113. https://doi.org/10.1016/j.jconrel.2014.12.008.

Pisani, S., Di Martino, D., Cerri, S., Genta, I., Dorati, R., Bertino, G., Benazzo, M., Conti, B., 2023. Investigation and Comparison of Active and Passive Encapsulation Methods for Loading Proteins into Liposomes. Int. J. Mol. Sci. 24 https://doi.org/10.3390/ijms241713542.

Rebollo, R., Oyoun, F., Corvis, Y., El-Hammadi, M.M., Saubamea, B., Andrieux, K., Mignet, N., Alhareth, K., 2022. Microfluidic Manufacturing of Liposomes: Development and Optimization by Design of Experiment and Machine Learning. ACS Appl. Mater. Interfaces 14, 39736–39745. https://doi.org/10.1021/acsami.2c06627.

Roces, C.B., Kastner, E., Stone, P., Lowry, D., Perrie, Y., 2016. Rapid quantification and validation of lipid concentrations within liposomes. Pharmaceutics 8, 1–11. https://doi.org/10.3390/pharmaceutics8030029.

Roces, C.B., Khadke, S., Christensen, D., Perrie, Y., 2019. Scale-Independent Microfluidic Production of Cationic Liposomal Adjuvants and Development of Enhanced Lymphatic Targeting Strategies. Mol. Pharm. 16, 4372–4386. https://doi.org/10.1021/acs.molpharmaceut.9b00730.

Roces, C.B., Lou, G., Jain, N., Abraham, S., Thomas, A., Halbert, G.W., Perrie, Y., 2020a. Manufacturing considerations for the development of lipid nanoparticles using microfluidics. Pharmaceutics 12, 1–19. https://doi.org/10.3390/pharmaceutics12111095.

Roces, C.B., Port, E.C., Daskalakis, N.N., Watts, J.A., Aylott, J.W., Halbert, G.W., Perrie, Y., 2020b. Rapid scale-up and production of active-loaded PEGylated liposomes. Int. J. Pharm. 586, 119566 https://doi.org/10.1016/j.ijpharm.2020.119566.

Rosa, A., Caprioglio, D., Isola, R., Nieddu, M., Appendino, G., Falchi, A.M., 2019. Dietary zerumbone from shampoo ginger: New insights into its antioxidant and anticancer activity. Food Funct. 10, 1629–1642. https://doi.org/10.1039/c8fo02395f.

Shah, S., Dhawan, V., Holm, R., Nagarsenker, M.S., Perrie, Y., 2020. Liposomes: Advancements and innovation in the manufacturing process. Adv. Drug Deliv. Rev. 154–155, 102–122. https://doi.org/10.1016/j.addr.2020.07.002.

Shan, H., Sun, Q., Xie, Y., Liu, X., Chen, X., Zhao, S., Chen, Z., 2024. Dialysis-functionalized microfluidic platform for in situ formation of purified liposomes. Colloids Surfaces B Biointerfaces 236, 113829. https://doi.org/10.1016/j.colsurfb.2024.113829.

Shepherd, S.J., Issadore, D., Mitchell, M.J., 2021. Microfluidic formulation of nanoparticles for biomedical applications. Biomaterials 274, 120826. https://doi.org/10.1016/j.biomaterials.2021.120826.

Shi, H., Xie, Z., Cao, Y., Zhao, Y., Zhang, C., Chen, Z., Reis, N.M., Liu, Z., 2022. A microfluidic serial dilutor (MSD): Design optimization and application to tuning of liposome nanoparticle preparation. Chem. Eng. Sci. 263, 118080 https://doi.org/10.1016/j.ces.2022.118080.

Tehrani, S.F., Bharadwaj, P., Leblond Chain, J., Roullin, V.G., 2023. Purification processes of polymeric nanoparticles: How to improve their clinical translation? J. Control. Release 360, 591–612. https://doi.org/10.1016/j.jconrel.2023.06.038.

Tiboni, M., Tiboni, M., Pierro, A., Del Papa, M., Sparaventi, S., Cespi, M., Casettari, L., 2021. Microfluidics for nanomedicines manufacturing: An affordable and low-cost 3D printing approach. Int. J. Pharm. 599, 120464 https://doi.org/10.1016/j.ijpharm.2021.120464.

Tuckerman, M., Berne, B.J., Martyna, G.J., 1992. Reversible multiple time scale molecular dynamics. J. Chem. Phys. 97, 1990–2001. https://doi.org/10.1063/1.463137.

Van Der Spoel, D., Lindahl, E., Hess, B., Groenhof, G., Mark, A.E., Berendsen, H.J.C., 2005. GROMACS: Fast, flexible, and free. J. Comput. Chem. 26, 1701–1718. https://doi.org/10.1002/jcc.20291.

Webb, C., Khadke, S., Schmidt, S.T., Roces, C.B., Forbes, N., Berrie, G., Perrie, Y., 2019. The impact of solvent selection: Strategies to guide the manufacturing of liposomes using microfluidics. Pharmaceutics 11, 653. https://doi.org/10.3390/pharmaceutics11120653.

Webb, C., Forbes, N., Roces, C.B., Anderluzzi, G., Lou, G., Abraham, S., Ingalls, L., Ingalls, L., Marshall, K., Leaver, T.J., Watts, J.A., Aylott, J.W., Perrie, Y., 2020. Using microfluidics for scalable manufacturing of nanomedicines from bench to GMP: A case study using protein-loaded liposomes. Int. J. Pharm. 582, 119266 https://doi.org/10.1016/j.ijpharm.2020.119266.

Yusuf, A., Almotairy, A.R.Z., Henidi, H., Alshehri, O.Y., Aldughaim, M.S., 2023. Nanoparticles as Drug Delivery Systems: A Review of the Implication of Nanoparticles' Physicochemical Properties on Responses in Biological Systems. Polymers (basel). 15 https://doi.org/10.3390/polym15071596.

Zhang, G., Sun, J., 2021. Lipid in chips: A brief review of liposomes formation by microfluidics. Int. J. Nanomedicine 16, 7391–7416. https://doi.org/10.2147/IJN.S331639.

Zook, J.M., Vreeland, W.N., 2010. Effects of temperature, acyl chain length, and flow-rate ratio on liposome formation and size in a microfluidic hydrodynamic focusing device. Soft Matter 6, 1352–1360. https://doi.org/10.1039/b923299k.